Robust Islanding Detection in Microgrids Employing Rate of Change of Kinetic Energy Over Reactive Power

Robust Islanding Detection in Microgrids Employing Rate of Change of Kinetic Energy Over Reactive Power

Hasan Khosravi, Haidar Samet, *Member, IEEE*, and Mohsen Tajdinian

***Abstract*—This study tries to outline a comprehensive approach established on the kinetic energy of the distributed generations (DGs) for islanding mode detection in micro-grids. More specifically, the proposed index calculates the rate of change of kinetic energy over reactive power (ROCOKORP) for each DG at the point of common coupling (PCC). Despite the islanding detection being the most challenging issue during complete match between the load and generation of DGs, the proposed method can swiftly deal with such an issue, therefore confirming its superiority. Other challenging conditions where islanding detection can either be difficult or confused with other events such as loads inside the non-detection zone (NDZ), various fault types, and loads at various power factors have also been considered to investigate the effectivity of the proposed approach. The proposed method's performance has been verified and evaluated in comparison to the state-of-the-art via a simulation testbed.**

***Index Terms*—Renewable energy resources, islanding, distributed generation, kinetic energy.**

I. Introduction

A. Motivation and Incitement

THE RENEWABLE energy -based distributed generation (DG) has drawn a lot of attention from the power industry researchers, as a solution for environmental concerns. However, the integration of networks with DGs is associated with many protection and security issues. One of these issues, called the islanding condition, prevails as the DGs continue to operate during service disconnection in power grids. Such a phenomenon may result in several problems, e.g., stability and power quality deterioration as the DGs may be incapable of standalone voltage and frequency preservation. Considering the detrimental effects of the unscheduled islanding, as a consequence of high DG penetration [1], [2], such an event is crucial to detect.

Manuscript received December 29, 2020; revised May 2, 2021 and September 3, 2021; accepted October 9, 2021. Date of publication October 13, 2021; date of current version December 23, 2021. Paper no. TSG-01923-2020.R2. *(Corresponding author: Haidar Samet.)*

Hasan Khosravi and Mohsen Tajdinian are with the School of Electrical and Computer Engineering, Shiraz University, Shiraz 7134851154, Iran.

Haidar Samet is with the School of Electrical and Computer Engineering, Shiraz University, Shiraz 7134851154, Iran, and also with the Department of Electrical Engineering, Eindhoven University of Technology, 5612 AZ Eindhoven, The Netherlands (e-mail: samet@shirazu.ac.ir).

Color versions of one or more figures in this article are available at https://doi.org/10.1109/TSG.2021.3119644.

Digital Object Identifier 10.1109/TSG.2021.3119644

B. Literature Review

The islanding phenomenon has been addressed in multiple technical standards including UL 1741 and IEEE 1547 [3], [4]. Along with the standards, the islanding phenomenon has been detected via different approaches over the years. Table I represents the four categories imaginable for the existing islanding detection approaches, given by remote- and local- control, artificial intelligence, and signal processing. The operation principle for the first group of methods, i.e., remote control -based, is laid on the analysis of DGs connecting to the main grid. Despite the good performance achieved via such an approach, they are also very costly to apply. The supervisory control and data acquisition (SCADA) system is a well-known example of a remote-control approach, which performs based on the regular analysis of conditions prone to islanding. As for another remote-control method, there can be the connection of DGs via transmission lines [5]. Through the remote-control methods, the system parameters, e.g., voltages and frequencies, are not monitored regionally, and thus are the local-control methods introduced to attain such an end.

The local-control approaches are generally carried out via three groups of passive algorithm (PA), active algorithm (AA), and hybrid algorithm (HA). The basis for passive techniques is laid on measuring certain system parameters. Nevertheless, system parameters may not be notably deviated for islanding condition to be detected in case of high equilibrium between the DG power and the load demand. On this ground, the sole depending on the parameter deviations cannot provide a reliable indication of islanding mode occurrence. Several examples for passive methods are including Over/Under voltage and frequency and phase jump detection (PJD) [6], rate of change of frequency (ROCOF) [7], inverse hyperbolic secant function (IHSF) [8], rate of change of frequency over reactive power (ROCOFORP) [9], rate of change of sequence components of current [10] and rate of change of phase angle difference(ROCPAD) [11].

In order to deal with the shortcomings of the passive techniques, most importantly the condition of load demand and DG generation equality, the active techniques have been proposed alternatively. The active methods operate based on the analysis of system response to an injected disturbance. The basic principle for such a technique is that an islanded system responds to a small disturbance by large variations, whereas the response of an interconnected network would not be

significant. However, there are also several disadvantages associated with these methods including the need for injecting a disturbance, deterioration of power quality, and slow decision-making considering the duration required for the system response analysis. Furthermore, the disturbances being applied to the system on a regular basis to check the islanding condition, are most of the time unnecessary. Several examples for the active methods are including active ROCOF [12], sliding mode frequency shift (SMFS) [13], active and reactive power control loops for synchronous machine DGs [14]. By combining the active and passive methods, their advantages can be achieved altogether via hybrid islanding detection techniques. Some examples of the hybrid methods are including Parallel inductance switching [15], Reactive power disturbance with three passive IDMs [16].

On another group of methods, the capabilities of artificial intelligence (AI) are applied to the passive islanding detection approaches. Although the AI-based techniques ensure islanding detection with a high level of accuracy [17], they are however time-consuming to train and practically inapplicable. Several AI-based approaches used for islanding detection are adaptive neuro-fuzzy inference system (ANFIS) [18], support vector machine classifier (SVM) [19], combination of an optimal Artificial Neural Network (ANN) based on Particle Swarm Optimization (PSO) with a simple active method [20], deep learning [21]. These methods mostly require high amount of training data and it may vulnerable to topology changes in the power system.

Likewise, several studies have been carried out on the application of signal processing (SP) with passive islanding detection methods to decrease their NDZ. Through SP approaches, the features of system parameter signals can be derived which are hidden from the typical passive methods. The most popularly used SP approaches for islanding detection are: variational mode decomposition (VMD) [22], transient monitoring function (TMF) [23], Matrix Pencil (MP) [24], intrinsic time decomposition (ITD) [25]. Even though the islanding detection accuracy is ensured by a high level via SP methods, the NDZ might not be practically minimized in the presence of highly complex DGs in the grid. The SP-based algorithms mostly suffer from high-sampling frequency, noisy condition, threshold setting, and pre-defined parameters.

In summary, some passive islanding detection approaches (i.e., groups 1 & 2 in Table I) are unable to effectively deal with the situation of equality between the generated power of DGs and the consumed power of loads. Although this problem has been dealt with by some the passive (i.e., group 3 in Table I) and active methods, the active approaches also endanger the power quality of the system through mostly unnecessary disturbance injections. The hybrid approaches offer more reliable and efficient performance with respect to the active and passive methods, although entailing longer detection time and heavier calculation burden. With the incorporation of signal processing and artificial intelligence into passive-based approaches, higher accuracies can be achieved. On the other hand, the AI-based methods' requirement to be re-trained, and the potential inability of SP-based methods in NDZ minimization is the most substantial deficiency of these approaches. Also, most of the algorithms may experience maloperation during non-islanding situations including different types of load switching and short circuit fault conditions.

TABLE I
VARIOUS ISLANDING DETECTION METHODS

Islanding detection technique		Advantages	Disadvantages	Ref.
Remote control		- High accuracy - Reliable	- Very high costs, especially in small networks	[5]
Local control	PA1*	- Low detection time - No disturbances applied to the system	- Big NDZ region - Complicated threshold defining	[6, 7]
	PA2*	- High accuracy in case of unbalance between generation and consumption	- Complicated threshold defining	[8, 9]
	PA3*			[10-11]
	AA	- Small NDZ region	- Disturbance injection to the system - Degraded power quality - Low detection speed due to time interval required for system response analysis	[12-14]
	HA	- Small NDZ region - Applying disturbances only when required	- high detection time	[15-16]
Artificial intelligence algorithms		- High precision - Good reliability	- More time to train the relevant data - Difficult to implement in practice	[17-21]
Signal Processing		- Low detection time - No disturbances applied to the system - Small or Zero NDZ	- High-sampling frequency - Poor response in noisy condition	[22-25]

* PA1: Traditional passive method with large NDZ, PA2: Modern passive method with small NDZ, PA3: Modern passive method with zero NDZ

C. Contribution and Paper Organization

This paper puts forward a novel approach based on the kinetic energy for the detection of islanding condition in the micro-grids. The presented approach is able to deal with islanding detection problem considering different types of DGs. The paper has the following contributions:

1) This paper introduces a new index based on the rate of change of kinetic energy over reactive power (ROCOKORP) for each DG at the PCC point. Kinetic energy for rotational DGs can be easily obtained through the swing equation. However, for inverter-interfaced DGs, the concept of the virtual synchronous generator can be employed to extract the kinetic energy term of these DG types.
2) Based on the ROCOKORP, an islanding detection criterion is derived which is designed based on the signal energy of ROCOKORP. The proposed criterion can swiftly discriminate the islanded condition from grid-connected mode within a short period even under a perfectly matched load and generation. As a result, unlike the passive methods in [6], [7], the proposed islanding detection criterion has zero NDZ.
3) Unlike [6]–[11], the proposed islanding detection is able to robustly operate under various islanding and non-islanding conditions including RLC load with different

quality factors, various types of the short circuit fault, load switching and capacitor switching.

4) Concentrating on mathematical complexity of the proposed criterion, it can be observed that the proposed method is very low complexity in comparison with AI based algorithms [17]–[21].

This paper is put forward by means of the following organization: in Section II the proposed islanding detection algorithm and its requirements for implementation are introduced. Section III provides various simulation results for the performance evaluation of the proposed method. Finally, the conclusion is provided in Section IV.

II. Proposed Islanding Detection Algorithm

In the following, mathematical basis of the calculation of the proposed index (PI) for islanding detection is described.

A. Rate of Change of Kinetic Energy

The operation of power systems demands that the generated and consumed power be equal. In the abnormal condition, rotating electrical machines either accelerate or deaccelerate in response to the increase or decrease of the rotor speed. To be specific, when the generation surpasses consumption, the power surplus is stored in the form of speed increase characterized in accelerated machines, and the opposite can be imagined for generation shortage. The kinetic energy (KE) produced in the rotating masses of electrical machines due to their speed changes can be expressed as [26]:

$$\mathrm{KE} = \frac{1}{2}\mathrm{J}\omega^2 \tag{1}$$

where J is the rotor moment of inertia and ω denotes angular frequency.

According to (1), the rate of change of KE (ROCOKE) is calculated as follows:

$$\frac{\mathrm{dKE}}{\mathrm{dt}} = \frac{\mathrm{d}\left(\frac{1}{2}\mathrm{J}\omega^2\right)}{\mathrm{dt}} = \frac{1}{2}\mathrm{J}\frac{\mathrm{d}\left(\omega^2\right)}{\mathrm{dt}} = \mathrm{J}\omega\dot{\omega} \tag{2}$$

As one can see in (2), ROCOKE is related to $\dot{\omega}$. During normal operation of the power grids, $\dot{\omega}$ is negligible and as a result, the ROCOKE value is close to zero. But during abnormal operation, the imbalance between power generation and consumption may result in rotor speed variations and accordingly, ROCOKE takes notable values. However, small power mismatch between generation and consumption in islanded area may result in small variations in rotor speed and consequently small value of ROCOKE. In order to create an index that detects islanding in all scenarios especially in small power mismatch, different power system parameters based on ROCOKE have been selected. Table II lists details of these parameters. The sensitivity of these parameters has been analyzed under various islanding and non-islanding scenarios as shown in Table III. The effectivity of each index has been analyzed using a MATLAB simulation of the micro-grid depicted in Fig. 1. The specifications of the adopted test system are provided in the Appendix.

Table IV shows the maximum value of each index for islanding and non-islanding scenarios shown in Table III after ignoring the initial transients. According to Table IV, dk/dp, dk/dq and dv/dk show significant changes during the islanding scenarios. However, if the behaviors of these parameters are compared with non-islanding events, only dk/dq has the best performance. To avoid the impact of initial transients on the islanding detection procedure, an index will be introduced in the following.

TABLE II
Different Power System Parameters Based on Rocoke

Number	Passive parameter
1	Rate of change of kinetic energy over active power (dk/dp)
2	Rate of change of active power over kinetic energy (dp/dk)
3	Rate of change of kinetic energy over reactive power (dk/dq)
4	Rate of change of reactive power over kinetic energy (dq/dk)
5	Rate of change of kinetic energy over voltage (dk/dv)
6	Rate of change of voltage over kinetic energy (dv/dk)

TABLE III
Various Events for Sensitivity Analysis

Event	Scenarios
Islanding	$\Delta P = 0\%$ to 2% and $\Delta Q = 0\%$ to 2%
Non-Islanding	Connecting and disconnecting a 500 KVAR capacitor bank
	Starting a 400 KVA induction motor
	Various type of faults with $R_f = 1\Omega$

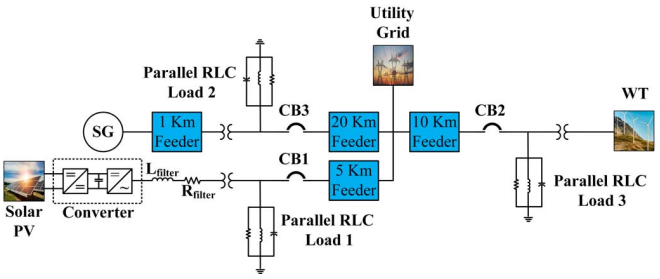

Fig. 1. The test system.

TABLE IV
Maximum Value of Each Index for Different Events

Type of DG	Event	dk/dp	dp/dk	dk/dq	dq/dk	dk/dv	dv/dk
PV	Islanding	62.5	2.27	102.5	15	3.26	87.5
	Non-Islanding	73.5	23.45	12.44	52.47	54.4	88.3
WT	Islanding	40.38	0.98	64.6	8.075	2.975	51.85
	Non-Islanding	47.27	8.221	4.158	31.62	38.81	60.23
SG	Islanding	55.18	1.72	81.96	8.036	4.286	72.32
	Non-Islanding	56.65	29.76	5.213	43.49	48.9	84.42

B. Rate of Change of Reactive Power

The power system in Fig. 2, consisting of a DG, a load unit, and an equivalent source representing the power grid, is a simple test system used for islanding studies. The load unit is conventionally considered as an RLC equivalent in islanding

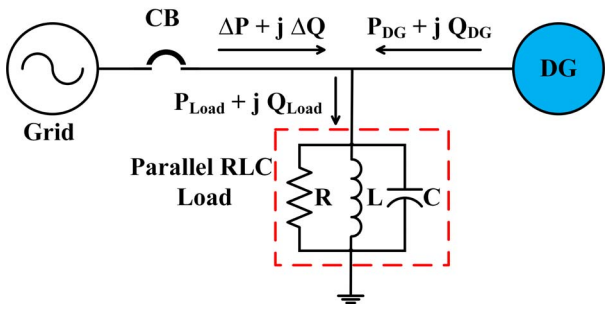

Fig. 2. Simple network with a grid-connected DG for studying the islanding.

detection studies [27]. The reactive power of the DG unit when operating in the grid-connected mode (the CB in Fig. 2 being closed) can be obtained as:

$$Q_{DG} + \Delta Q = Q_{Load} \Longrightarrow Q_{DG} = V^2\left(\frac{1}{\omega L} - \omega c\right) - \Delta Q \quad (3)$$

where V is the magnitude voltage at PCC bus, Q_{DG} is the reactive power of DG, Q_{load} is the reactive power of load. In addition, L and C are inductance and capacitance of the RLC load shown in Fig. 2. If islanding occurs (the CB in Fig. 2 being open), the reactive power injected by the upstream network is zero ($\Delta Q = 0$). As a result, the reactive power of a DG is calculated as follows:

$$Q_{DG} = V^2\left(\frac{1}{\omega L} - \omega c\right) \quad (4)$$

According to (4), the rate of change of reactive power (ROCORP) of DG is obtained as follows:

$$\frac{dQ_{DG}}{dt} = 2V\dot{V}\left(\frac{1}{\omega L} - \omega c\right) - V^2\left(\frac{\dot{\omega}}{\omega^2 L} + \dot{\omega} c\right) \quad (5)$$

where $\dot{V}$ and $\dot{\omega}$ are the derivation of V and ω respectively.

Equations (3) to (5) have been brought just for description of reactive power for RLC load shown in Fig. 2. In practice, the ROCORP has been calculated based on "Recursive Formula" as follows [28]:

$$Q(t) = Q(t - \Delta t) + \frac{2\Delta t}{T}\left(R(t) - R\left(t - \frac{T}{2}\right)\right) \quad (6)$$

$$R(t) = v\left(t - \frac{T}{4}\right) i(t) \quad (7)$$

$$\frac{dQ}{dt} = \frac{Q(t) - Q(t - \Delta t)}{\Delta t} = \frac{2}{T}\left(R(t) - R\left(t - \frac{T}{2}\right)\right). \quad (8)$$

C. Calculating Energy of Rate of Change Kinetic Energy Over Reactive Power

The PI is introduced as the integral of the absolute squares of the ROCOKORP over half fundamental period T. The latter sentence is mathematically calculated as follows:

$$PI = \frac{1}{T/2}\int_{T/2}\left|\frac{dKE/dt}{dQ/dt}\right|^2 dt = \frac{2}{T}\int_{T/2}\left|\frac{dKE}{dQ}\right|^2 dt \quad (9)$$

The integration interval must be selected appropriately so that the proposed method has high reliability and low time delay. To such aim, three integration intervals have been selected.

TABLE V
SPECIFICATIONS OF DIFFERENT INTEGRATION INTERVAL

Integration interval	T/4	2T/4	3T/4
Difference between islanding and non-islanding events	1 analyzing window with length of T/4	2 analyzing windows with total length of 4T/4	2 analyzing windows with total length of 6T/4
Time delay	7×T/4=7T/4	5×2T/4=10T/4	4×3T/4=12T/4

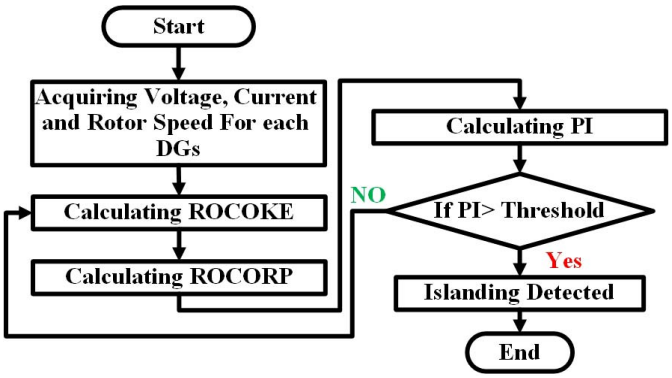

Fig. 3. Implementation stages of the proposed islanding detection algorithm.

Table V shows the specifications of all integration intervals briefly. According to Table V, by selecting the integration interval equals to T/4, the reliability of the proposed method decreases (the difference between islanding and non-islanding is 1 analyzing window with length of T/4). However, by selecting the integration interval equals to 3T/4, also the reliability of the proposed method increases (the difference between islanding and non-islanding is 2 analyzing windows with total length of 6T/4) but the proposed method will have more time delay. Therefore 2T/4 has been selected for integration interval.

D. Implementation of the Proposed Algorithm

The procedure of the proposed algorithm is shown in Fig. 3. The steps of the proposed method algorithm are as follows:

1) The voltage, current and rotor speed of each DG are acquired.
The frequency of the sampling rate is selected 6 kHz.
2) The ROCOKE ($\frac{dKE}{dt}$) is calculated using (2).
3) The ROCORP ($\frac{dQ_{DG}}{dt}$) is calculated using (8).
4) PI is calculated using (9). Note that if the PI exceeds the threshold for 5 consecutive samples, islanding is identified.

III. SIMULATION RESULTS AND DISCUSSIONS

The effectivity of the proposed approach has been analyzed using the micro-grid shown in Fig. 1.

A. Selecting the Threshold

A comprehensive method for islanding detection must be also capable of distinguishing several other system conditions such as short circuits, switching of loads, starting of motors, and switching of capacitor banks. Consequently, the threshold must be defined appropriately for the islanded condition to be discriminated from other similar events. To such aim,

TABLE VI
DIFFERENT TYPE OF ISLANDING AND NON-ISLANDING EVENTS

No.	Event	Parameters and their variation	Test cases
1	Islanding	$\Delta P = -75\%$ to 50% $\Delta Q = -20\%$ to 20%	100
2	Faults on 20, 40, 60 and 80% of distribution feeder	Types of fault = LG, LL, LLG, LLL, LLG	400
		$R_f = 0.5\ \Omega - 10\ \Omega$ in steps of $0.5\ \Omega$	
3	Motor Starting	10 – 300 KVA in steps of 10KVA	30
4	Capacitor Switching	Connecting and disconnecting from 40 – 400 KVAR in steps of 10 KVA	20
5	Linear and Non-Linear Load Switching	Connecting and disconnecting from 40 – 400 KVAR in steps of 10 KVA	40
6	Sudden change of Load PF	0.55 Lag – Unit PF in steps of 0.05	10
Total number of test cases			**600**

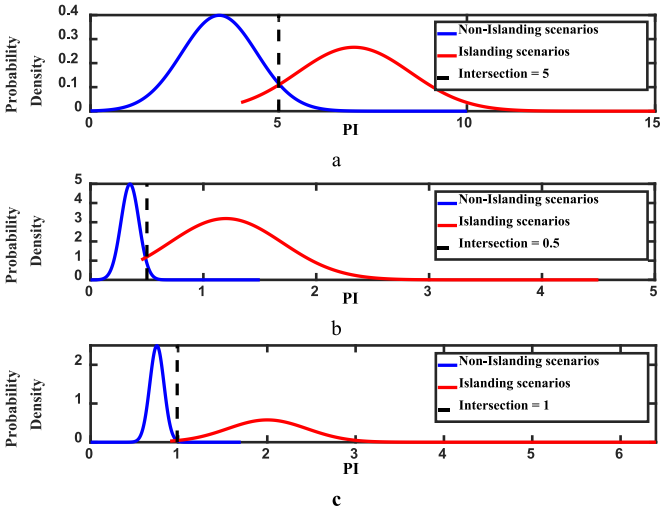

Fig. 4. PDFs for the PI in the first half-cycle and the selected threshold, (a) for PV, (b) for WT, (c) for SG.

an algorithm named "*Otsu thresholding method*" has been utilized which is a well-known and reliable method, employed in different engineering fields [29]. In the following, implementation of *Otsu thresholding method* in the proposed method is described in more details.

1) In the first step, a Probability Function Density (PDF) is assigned to a desired parameter for different conditions such as islanding and non-islanding scenarios which are tabulated in Table VI. (in the proposed method, PDFs should be assigned for index PI)
2) In the second step, a normal function based curve should be fitted for each case.
3) In the third step, the intersection point of the PDF curves regarding the islanding and non-islanding cases is selected as the threshold value.

As one can see in Fig. 4, the PDFs of the PI for islanding and non-islanding have intersection at 5, 0.5 and 1 for PV, WT and SG respectively. As a result, 5, 0.5 and 1 are considered as the threshold for PV, WT and SG respectively. According to

TABLE VII
NUMBER OF CONSECUTIVE SAMPLES OF PI THAT CROSSES THE THRESHOLDS

Type of DG	Operating Condition			
	Islanding		Non-Islanding	
	Min.	Max.	Min.	Max.
PV	6	63	0	3
WT	6	71	0	3
SG	5	54	0	3

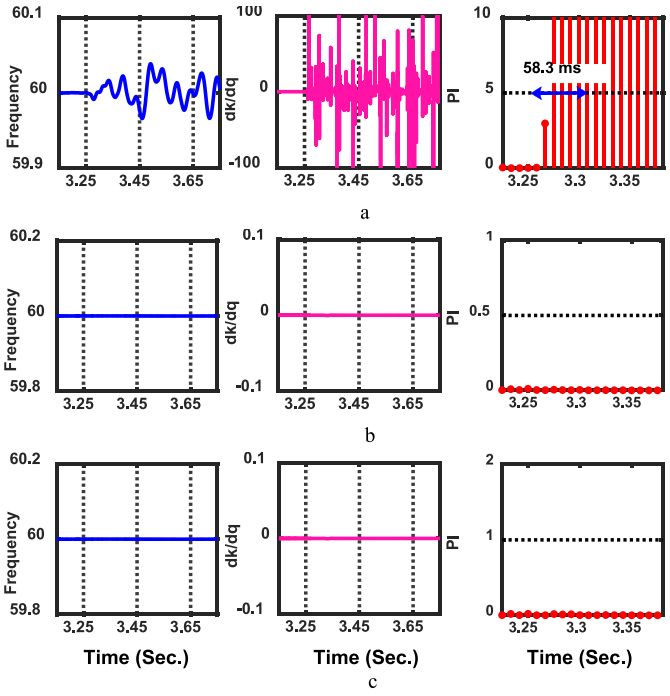

Fig. 5. Performance evaluation of the proposed method when there is a full balance between load and generation, (a) PV panel, (b) Wind turbine, (c) Synchronous generator.

Fig. 4, the PI of different types of DGs may have much higher value than their thresholds for non-islanding conditions due to initial transients. Therefore, an extra criterion (i.e., 5 consecutive samples of PI) has been considered for decision making. "5 consecutive samples of PI" is acquired via simulation of various cases as in Table VI at t = 3.25s. Table VII shows the maximum and minimum number of consecutive samples of PI that crosses the thresholds from t = 3.25s until t = 4.25s. According to Table VII, the maximum number of consecutive samples of PI that crosses the thresholds in non-islanding scenarios is 3. However, the minimum number of consecutive samples of PI that crosses the thresholds in islanding scenarios is 5. Therefore, if the PI remains higher than the thresholds for 5 consecutive samples of PI, the islanding is detected. On the contrary, if the PI does not remain higher than the thresholds for 5 consecutive samples of PI, the condition is not considered as an islanding case.

B. Performance Evaluation Considering the Full Balance Between Load and Generation

To investigate the performance of PI in the case of full balance between load and generation, three cases are provided in Figs. 5 to 7. In Fig. 5, PV and its RLC load become islanded

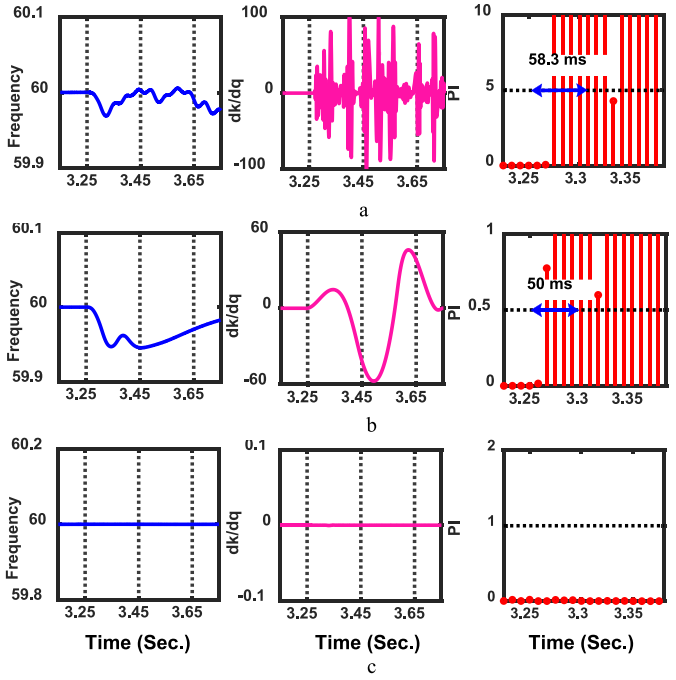

Fig. 6. Performance evaluation of the proposed method when there is a full balance between load and generation, (a) PV panel, (b) Wind turbine, (c) Synchronous generator.

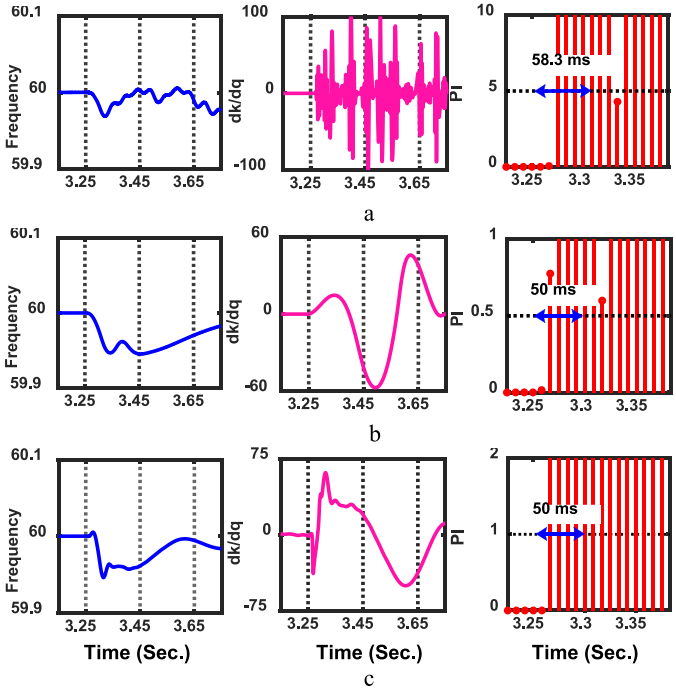

Fig. 7. Performance evaluation of the proposed method when there is a full balance between load and generation, (a) PV panel, (b) Wind turbine, (c) Synchronous generator.

once the CB1 is opened at t = 3.25s. Note that CBs 2 and 3 are closed during this condition. As one can see in Fig. 5, the frequency of SG and WT are almost constant and the PI is less than the threshold for these two DGs. However, although the frequency of PV is in the allowable range, the PI index detects islanding condition in 58.3 ms for the PV.

In Fig. 6, CBs 1 and 2 are opened at t = 3.25 s and CB3 remains closed. Similar to the previous case, the PI crosses the threshold for PV and WT for 5 consecutive samples of PI after 58.3 ms and 50 ms, respectively. As a result, the PI determines the islanding of PV and WT. For SG, PI remains below the threshold and as a result, the PI does not detect islanding mode for SG. In Fig. 7, CBs 1 to 3 are opened at t = 3.25 s. As shown in Fig. 7, the PI goes upper than the threshold for all DGs for 5 consecutive samples of PI after almost 50 ms.

C. Performance Evaluation Under UL 1741 Standard

To verify the credibility of the proposed approach, its performance is confirmed in accordance with the technical standard of UL 1741 [4]. Therefore, the active power consumption of the loads is to be changed within 25, 50, 100, and 125% of the generated active power from the inverter of the PV unit. The reactive power consumption of the loads can also be varied within the interval of 95% to 105% by 1% steps while preserving a unity power factor. According to Fig. 8, the performance of the PI is evaluated for two following conditions: 1) 15% active power unbalance and full balance in reactive power, and 2) 1% reactive power unbalance and full balance in active power. As it can be seen in Fig. 8, the PI identifies islanding for all DGs since the PI crosses the thresholds for 5 consecutive samples. As one can see in Fig. 8.a, the maximum islanding detection time is 58.3 ms.

TABLE VIII
NDZ REGION OF VOLTAGE AND FREQUENCY RELAYS FOR 3 DGS

Type of DG	PV	WT	SG
△P (KW	[-43.5 72]	[-60 50]	[-24 20]
△Q (KVAR)	[-9.05 4.173]	[-17.815 12.348]	[-7.119 4.935]

D. Performance Evaluation for Loads in NDZ Region of Voltage and Frequency Relays

This section is dedicated to functionality of the PI in NDZ. The calculation details of NDZ for voltage and frequency relays have been provided in [30]. Typically, the permissible range for voltage and frequency in a distribution system are between 0.88 to 1.1 p.u and 59.3 to 60.5 Hz, respectively. Table VIII represents the obtained NDZ of voltage and frequency relays for the imbalance of active and reactive power regarding the 3 DGs under study. The proposed approach has been tested on 2 cases to analyze its performance upon load variation in the grid's NDZ, as shown in Fig. 9. It is noteworthy that the voltage and frequency stay within the permissible variation limits only in two cases, thus confirming the inability of conventional relays to identify islanding in such conditions. In order to account for a challenging scenario of islanding detection, the proposed technique is tested by considering some levels of active power imbalance while holding the reactive power at full balance. The active power is assumed to be out of balance by −5 kW, and 10 kW, while preserving the reactive power balance. It is depicted in Fig. 9 that the PI can

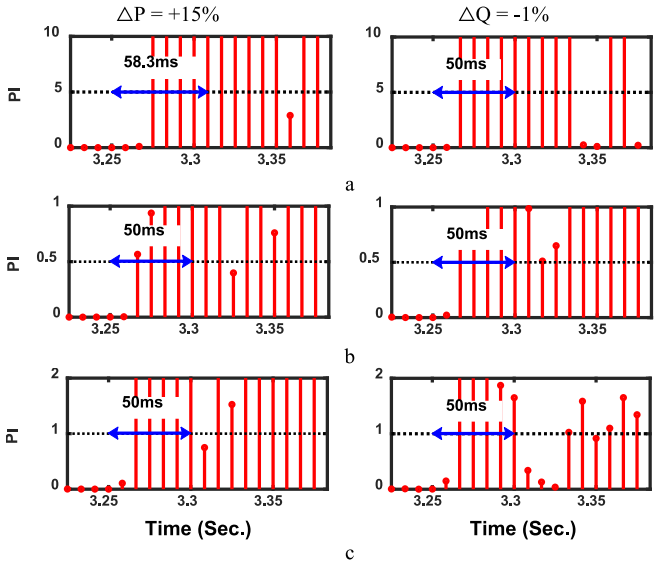

Fig. 8. Performance evaluation under UL 1741 standard, (a) PV panel, (b) Wind turbine, (c) Synchronous generator.

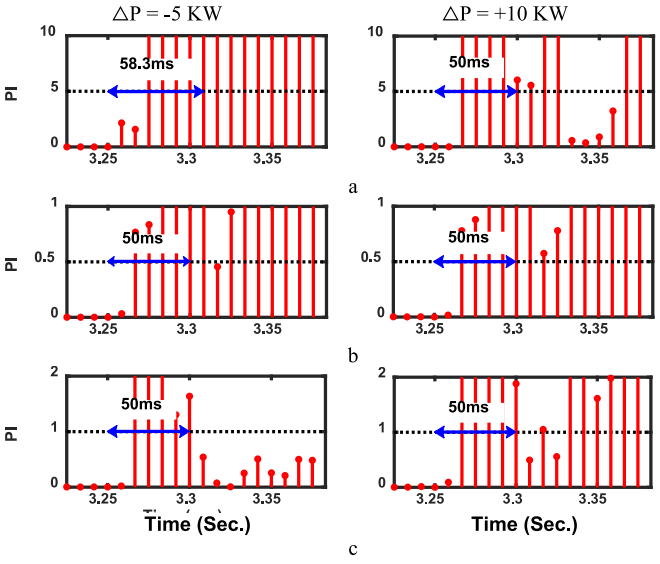

Fig. 9. Performance evaluation for loads in NDZ region of voltage and frequency relays, (a) PV panel, (b) Wind turbine, (c) Synchronous generator.

accurately determine the islanding in under 58.3 ms after its occurrence.

E. Performance Evaluation for Load Quality Factor

Here, the proposed approach is tested for different quality factors under nominal loading, according to standard UL 1741 [4], instructing for the quality factor (Q_f) under 2.5. Furthermore, the generation and consumption have also been set in full balance. Accordingly, two islanding conditions have been produced by opening the CBs at t = 3.25 s, considering Q_f equals to 2 and 2.5. As can be seen in Fig. 10, the PI can determine islanding occurrence in under 58.3 ms, subsequent to event inception.

F. Performance Evaluation for Load Switching

In this section, the proposed method is evaluated in the presence of the switching of various linear and nonlinear loads.

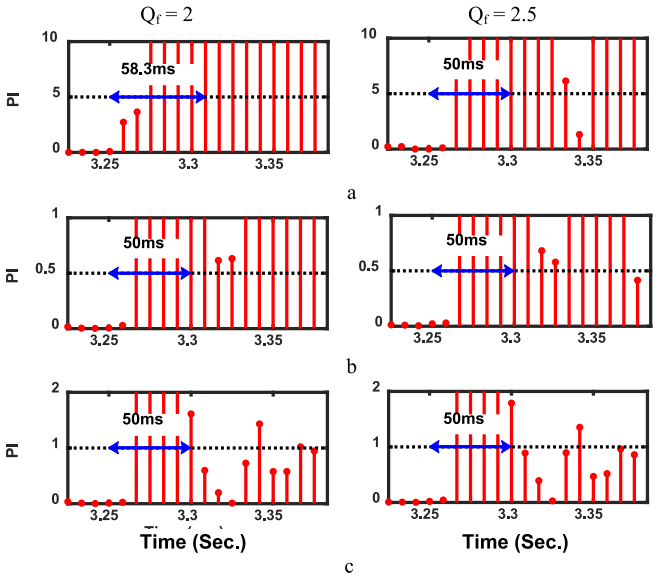

Fig. 10. Performance evaluation for load Quality Factor, (a) PV panel, (b) Wind turbine, (c) Synchronous generator.

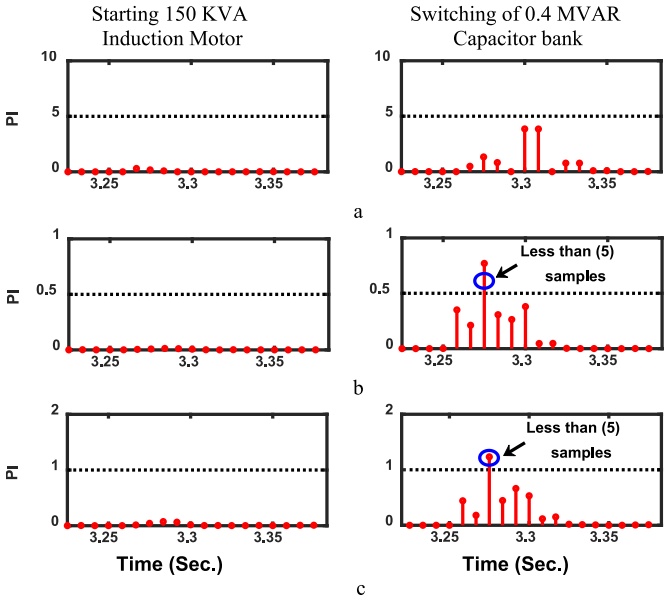

Fig. 11. Performance evaluation for load switching, (a) PV panel, (b) Wind turbine, (c) Synchronous generator.

Here, the induction motor starting and capacitor bank switching have been considered. It is clearly visible in Fig. 11 that the proposed index does not remain above the determined threshold for five consecutive samples in response to load switching.

G. Performance Evaluation for Short Circuit Faults

Here, the proposed algorithm is tested in the face of short circuit occurrence in the network. The short circuit incepts at t = 3.25 and persists for 0.1 s. As depicted in Fig. 12, the PI does not stay above the predetermined threshold for more than 5 consecutive energy samples.

H. Evaluation on IEEE 33-Bus Distribution System

The performance evaluation of the presented method has been verified on IEEE 33-bus distribution system. The

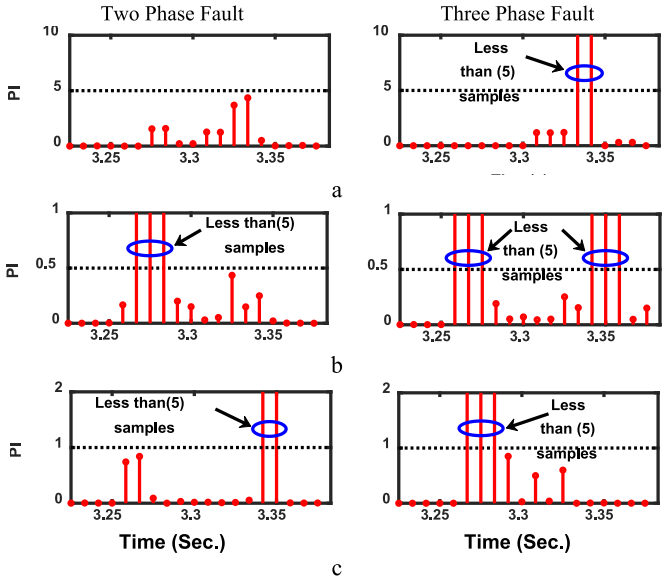

Fig. 12. Performance evaluation for short circuit faults, (a) PV panel, (b) Wind turbine, (c) Synchronous generator.

TABLE IX
OUTPUT RESULTS OF PROPOSED METHOD FOR ISLANDING CONDITION IN IEEE 33-BUS DISTRIBUTION NETWORK

△P (%)	△Q (%)	No. of consecutive samples of PI: larger than (7.25) for PV	larger than (0.8) for WT	larger than (1.2) for SG	△P (%)	△Q (%)	No. of consecutive samples of PI: larger than (7.25) for PV	larger than (0.8) for WT	larger than (1.2) for SG
-20	-10	8	13	10	4	-10	7	6	8
	-5	9	9	11		-5	8	11	13
	0	14	10	8		0	10	9	13
	5	11	13	13		5	7	8	14
	10	6	13	11		10	10	13	13
-12	-10	6	13	11	12	-10	10	10	14
	-5	13	13	7		-5	14	7	10
	0	10	6	8		0	7	10	8
	5	14	11	14		5	7	9	9
	10	6	12	10		10	8	14	13
-4	-10	11	14	14	20	-10	12	11	9
	-5	8	13	8		-5	6	12	13
	0	9	9	6		0	8	8	10
	5	14	7	7		5	12	7	10
	10	12	11	9		10	6	12	8

specifications and topology of the test system are adopted from [31]. To create a loop in the test system, the sectionalizing switch 25 has been opened and the tie switches 36 and 37 have been closed. Three DG units (i.e. SG, PV and WT) are placed at buses 18, 22, and 25 with active power capacities of 0.5, 2.5 and 0.6 MVA. Similar to the test system shown in Fig. 1, using more than 1000 different islanding and non-islanding events, the threshold in IEEE 33 bus network for PV, WT and SG are selected 7.25, 0.8, and 1.2 respectively. Some simulation results have been numerically provided in Tables IX and X. By opening Sectionalizing switch 1 at t = 3.25 s, all DGs become islanded. The different imbalance level of active and reactive powers for islanding scenarios in Table IX are provided by changing the loads in network.

TABLE X
OUTPUT RESULTS OF PROPOSED METHOD FOR NON-ISLANDING CONDITION IN IEEE 33-BUS DISTRIBUTION NETWORK

Type	R_f (Ω)	No. of consecutive samples of PI: larger than (7.25) for PV	larger than (0.8) for WT	larger than (1.2) for SG	Type	Rang	No. of consecutive samples of PI: larger than (7.25) for PV	larger than (0.8) for WT	larger than (1.2) for SG
LLLG	0.1	2	2	2	SIM (hp)	750	0	0	0
	3.4	2	2	3		1500	1	1	0
	6.7	2	3	3		2250	2	2	0
	10	2	3	3		3000	2	2	1
LLG	0.1	0	2	2	CS (MVar)	0.5	1	1	1
	3.4	1	3	2		1	1	1	1
	6.7	0	3	2		1.5	2	2	2
	10	1	3	2		2	2	2	3
LG	0.1	0	2	1	NLL (MW)	0.5	1	1	1
	3.4	0	2	2		1	1	1	1
	6.7	1	3	2		1.5	2	2	1
	10	2	2	2		2	3	3	2

SIM: Switching Induction Motor, CS: Capacitor Switching, NLL: Non-Linear Load switching.

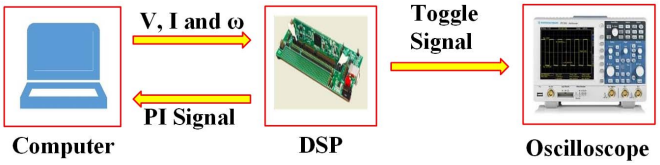

Fig. 13. The schematic of the employed test bench.

Tables IX and X show the maximum number of consecutive samples for PI from t = 3.25 s until t = 3.375 s. According to Table IX, the proposed method can detect the islanding conditions for different power mismatches. Also for non-islanding conditions, several scenarios are evaluated and shown in Table X. For this table, the fault events are applied between buses 2 and 3 at t = 3.25 s, and switching events are performed at bus 2. According to Table X, the proposed method can robustly deal with non-islanding conditions without experiencing mal-operation.

I. Experimental Validation of the Proposed Scheme

Experimental validation of the proposed scheme is carried out using DSP processor TMDSCNCD28335. According to Fig. 13, the test bench includes a computer with core i5-5200U CPU, a TMDSCNCD28335 board, and an oscilloscope to record the toggle signal. The processor has high-performance static CMOS technology – up to 150 MHz (6.67 ns Cycle Time). In addition, it includes 256K × 16 flash memory and 34K × 16 SARAM memory on the chip. During DSP implementation, the 4-bus test system shown in Fig. 1 with △P = 15% and △Q = 2% is simulated and the required signals (V, I and ω) are measured and saved. After that, this data is sent from PC to DSP, sample by sample through a serial communication link with a sampling frequency of 6 kHz. The DSP processes the received data and sends the PI signal to the computer. The toggle signal confirms that the processor can

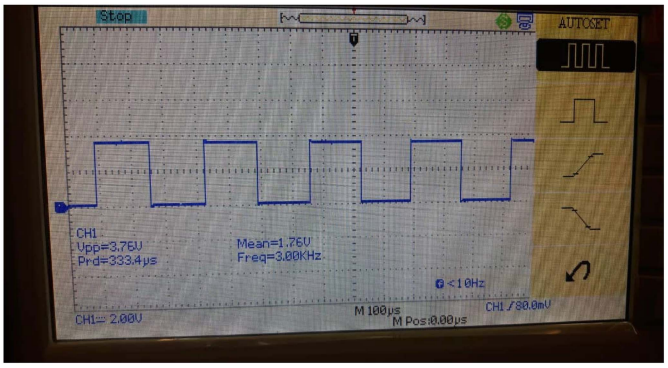

Fig. 14. Toggle signal of the proposed method.

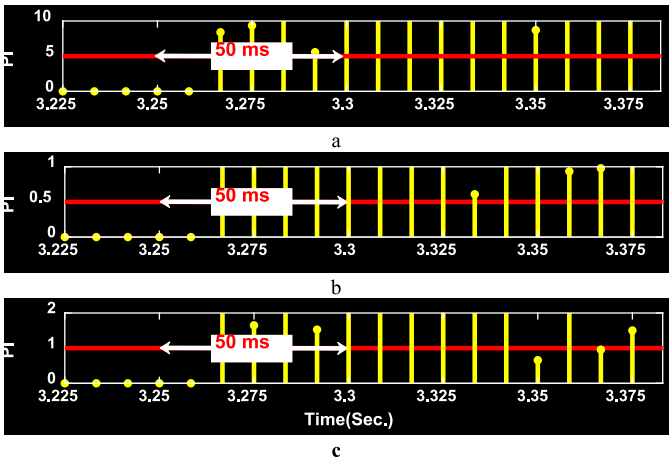

Fig. 15. Experimental validation of the proposed scheme, (a) PV panel, (b) Wind turbine, (c) Synchronous generator.

handle the calculations in real-time. Fig. 14 shows the toggle signal steps in each sampling period. According to Fig. 15, the PI identifies the islanding condition for all DGs in 50 ms.

J. Performance Comparison With Other Algorithms

Comparison with other techniques has been provided in three parts including NDZ, false detected zone (FDZ), and computational and operating time. All these cases have been simulated on IEEE 15 bus network.

1) NDZ: The performance of the PI is compared with voltage and frequency relay [6], rate of change of frequency (ROCOF) [7], inverse hyperbolic secant function (IHSF) [8], rate of change of frequency over reactive power (ROCOFORP) [9], rate of change of sequence components of current (ROCPSI/ROCNSI) [10] and rate of change of phase angle difference (ROCPAD) [11]. The results of these methods are tabulated in Table XI. To obtain the NDZ of the PI and methods [6]–[11], a large number of islanding cases were simulated with different values of active and reactive power unbalance (from -30% to 30% of active power mismatch and from -5% to 5% of reactive power mismatch in step of 0.2%). As it can be seen in Table XI, methods [10], [11] and the proposed methods have zero NDZ.

2) FDZ: Except Low NDZ, the immunity the islanding detection method against non-islanding situations must

TABLE XI
COMPARATIVE ASSESSMENT OF THE PROPOSED SCHEME

Method	NDZ (%)	LQF	Fault	CS	SIM	NLL	Accuracy (%)	DT (ms)	Big O	BT (µs)
Ref. [6]	*	✗	✗	✗	✓	✗	72.3	4-2000	O(n)	0.64
Ref. [7]	**	-	✗	-	✓	-	76.26	> 20	O(n)	0.71
Ref. [8]	5%	-	✓	✓	✓	-	90.83	> 135	O(n)	3.21
Ref. [9]	1.6%	✓	✓	✓	✓	-	96.4	200	O(n)	0.95
Ref. [10]	0 %	-	✓	✓	✓	-	91.19	20	O(n)	3.1
Ref. [11]	0 %	-	✗	✓	-	-	83.45	> 13	O(n)	2.96
Proposed Method	0 %	✓	✓	✓	✓	✓	99.28	50-58.3	O(n)	1.06

'√', '×' and '–' indicates operating condition verified, fails, and not considered, respectively. LQF : Load Quality Factor, CS: Capacitor Switching, SIM: Switching Induction Motor, NLL: Non-Linear Load switching, DT: Detection Time (ms), BT: Burden Time (µs), '*': $\Delta P = [-17.4\ 29.2]$, $\Delta Q = [-3.6\ 1.6]$,'**': $\Delta P = [-9\ 9]$, $\Delta Q = [-1\ 1]$

be preserved. To such aim, several non-islanding conditions have been applied to the proposed method and methods [6]–[11]. The accuracy of the methods is illustrated in Table XI. According to Table XI, the algorithms voltage and frequency relay [6], ROCOF [7], IHSF [8], ROCPSI/ROCNSI [10] and ROCPAD [11] cannot comprehensively deal with different non-islanding conditions and as a result, the accuracy of these methods are significantly less than the proposed method. These methods have accuracy between 72% to 91% for dealing with non-islanding conditions. While ROCOFORP [9] has robust performance in most cases and its accuracy is about 96% in non-islanding events. However, ROCOFORP has a long detection time. As a result, the proposed algorithm provides fast islanding detection with high precision and reliable operation during different non-islanding circumstances.

3) Computational and Operating Times: The computation complexity and burden time of the proposed method and the methods in [6]–[11] are shown in Table XI. The computation complexity has been provided based on big O notation. The concept of Big O notation is used to demonstrate the behavior of algorithm's run time while the input size grows [32]. Also the burden time can be calculated in MATLAB using "Tick Count" and "tic-toc" respectively. The calculations are conducted using a computer with core i5-5200U up to 2.7 GHz and 4GB memory in MATLAB. As it can be seen from Table XI, all methods have same computation complexity based on big O notation. However, considering both response time and burden time, [7], and the proposed method show the better performance comparing with the other methods.

K. Discussion on the Results and Main Achievements

In the previous sub-sections, the performance of the PI has been evaluated in various circumstances considering different test systems and furthermore compared with state-of-the-art algorithms. It is observed that:

1) The proposed method is able to deal with islanding detection of different type DGs. The islanding detection response time of synchronous generator, WT and PV is 50 and 58.3 ms respectively.

TABLE XII
MICROGRID SPECIFICATION

Component	Value	Component	Value
General Information			
Nominal Grid Voltage	25 KV	Nominal Grid Frequency	60 Hz
Load Quality Factor	1.5	Load Resonant Frequency	60 Hz
PV Panel			
DG Output Power	250 KW	PWM Carrier Frequency	1980 Hz
Input DG Voltage	480 V	Voltage (Ph-Ph)	250 v
Reference temperature	45°C	$R_{\text{Local load 1}}$	2.5 KΩ
$L_{\text{Local load 1}}$	4.421 H	$C_{\text{Local load 1}}$	1.59 μF
Synchronous Generator			
DG Output Power	200 KW	Voltage (Ph-Ph)	2200 v
Inertia Constant	0.8788 s	$R_{\text{Local load 2}}$	3.125 KΩ
$L_{\text{Local load 2}}$	5.53 H	$C_{\text{Local load 2}}$	1.237 μF
Wind Turbine			
DG Output Power	500 KW	Voltage (Ph-Ph)	575 v
Inertia Constant	0.685 s	$R_{\text{Local load 3}}$	1.25 KΩ
$L_{\text{Local load 3}}$	2.21 H	$C_{\text{Local load 3}}$	3.183 μF

2) The PI detects islanding condition considering RLC different load quality factors even in the case of full balance between load and generation.
3) Applying different fault type, load and capacitor switching and motor starting, it is observed that the PI has robust operation and does not experience mal-operation during non-islanding conditions.
4) Comparing with state-of-the-art algorithms, it can be observed that the PI and methods [10], [11] have zero NDZ.
5) In the case of robustness against non-islanding condition, Table XI indicates the PI has nearly 100% accuracy (or almost zero FDZ).
6) The result of the hardware validation shows the PI is suitable for real-time application.
7) Considering all the comparison's criteria together (i.e., NDZ, FDZ, DT, Big O and BT) in Table XI, the PI provides good response time and low computation complexity and simultaneously the highest accuracy among the methods.

IV. CONCLUSION

In this paper, a novel method has been established based on kinetic energy for detecting the islanding condition in micro-grids. The proposed method was formulated based on the ROCOKORP at the PCC of each DG. The proposed index can be applied for different types of DGs typically utilized in micro-grids. The ability of the proposed index to accurately determine the islanded and non-islanded modes within a short duration has been confirmed via numerous tests under various conditions. The results from simulations demonstrate that the proposed index is a comprehensive criterion for discrimination of islanded condition from other events which prevail during non-islanded operation. The proposed approach operates with a zero NDZ, even in the condition of consumption and generation full balance. Along with comprehensiveness, the proposed approach is easy to implement, acts with high precision, and is significantly fast in the detection of islanded mode occurrence. On this account, the proposed approach provides an applicable solution for islanding detection issue in the micro-grids.

APPENDIX

The specifications of the adopted test system in Table XII.

REFERENCES

[1] C. L. Trujillo, D. Velasco, E. Figueres, and G. Garcerá, "Analysis of active islanding detection methods for grid-connected microinverters for renewable energy processing," *Appl. Energy*, vol. 87, no. 11, pp. 3591–3605, Nov. 2010.

[2] F. Hashemi, N. Ghadimi, and B. Sobhani, "Islanding detection for inverter-based DG coupled with using an adaptive neuro-fuzzy inference system," *Elect. Power Energy Syst.*, vol. 45, no. 1, pp. 443–455, Feb. 2013.

[3] *IEEE Standard for Interconnecting Distributed Resources With Electric Power Systems*, IEEE Standard 1547-2008, 2008.

[4] *Standard for Inverters, Converters, Controllers and Interconnection System Equipment for Use With Distributed Energy Resources*, UL Standard 1741, Jan. 2010.

[5] S. K. G. Manikonda and D. N. Gaonkar, "Comprehensive review of IDMs in DG systems," *IET Smart Grid*, vol. 2, no. 1, pp. 11–24, Apr. 2019.

[6] M. Mishra, S. Chandak, and P. K. Rout, "Taxonomy of Islanding detection techniques for distributed generation in micro-grid," *Renew. Energy Focus*, vol. 31, pp. 9–30, Dec. 2019.

[7] W. Freitas, W. Xu, C. M. Affonso, and Z. Huang, "Comparative analysis between ROCOF and vector surge relays for distributed generation applications," *IEEE Trans. Power Del.*, vol. 20, no. 2, pp. 1315–1324, Apr. 2005.

[8] K. Sareen, B. R. Bhalja, and R. P. Maheshwari, "Islanding detection technique based on inverse hyperbolic secant function," *IET Renew. Power Gener.*, vol. 10, no. 7, pp. 1002–1009, Jul. 2016.

[9] S. Raza, H. Mokhlis, H. Arof, J. A. Laghari, and H. Mohamad, "A sensitivity analysis of different power system parameters on islanding detection," *IEEE Trans. Sustain. Energy*, vol. 7, no. 2, pp. 461–470, Apr. 2016.

[10] K. Sareen, B. R. Bhalja, and R. P. Maheshwari, "Universal islanding detection technique based on rate of change of sequence components of currents for distributed generations," *IET Renew. Power Gener.*, vol. 10, no. 2, pp. 228–237, Feb. 2016.

[11] A. Samui and S. R. Samantaray, "Assessment of ROCPAD relay for islanding detection in distributed generation," *IEEE Trans. Smart Grid*, vol. 2, no. 2, pp. 391–398, Jun. 2011.

[12] P. Gupta, R. S. Bhatia, and D. K. Jain, "Active ROCOF relay for islanding detection," *IEEE Trans. Power Del.*, vol.32, no.1, pp. 420–429, Feb. 2017.

[13] D. Voglitsis, F. Valsamas, N. Rigogiannis, and P. Nick, "On the injection of sub/inter-harmonic current components for active anti-islanding purposes," *Energies*, vol. 11, no. 11, p. 2183, Sep. 2018.

[14] R. Zamani, M. E. Hamedani-Golshan, H. H. Alhelou, S. Pierluigi, and R. P. Hemanshu, "Islanding detection of synchronous distributed generator based on the active and reactive power control loops," *Energies*, vol. 11, no. 10, p. 2819, Oct. 2018.

[15] A. Rostami, A. Jalilian, S. Zabihi, J. Olamaei, and E. Pouresmaeil, "Islanding detection of distributed generation based on parallel inductive impedance switching," *IEEE Syst. J.*, vol. 14, no. 1, pp. 813–823, Mar. 2020.

[16] X. Chen, Y. Li, and P. Crossley, "A novel hybrid islanding detection method for grid-connected microgrids with multiple inverter-based distributed generators based on adaptive reactive power disturbance and passive criteria," *IEEE Trans. Power Electron.*, vol. 34, no. 9, pp. 9342–9356, Sep. 2019.

[17] A. Khamis, Y. Xu, Z. Y. Dong, and R. Zhang, "Faster detection of microgrid islanding events using an adaptive ensemble classifier," *IEEE Trans. Smart Grid*, vol. 9, no. 3, pp. 1889–1899, May 2018.

[18] D. Mlakić, H. R. Baghaee, and S. Nikolovski, "A novel ANFIS-based islanding detection for inverter-interfaced microgrids," *IEEE Trans. Smart Grid*, vol. 10, no. 4, pp. 4411–4424, Jul. 2019.

[19] H. R. Baghaee, D. Mlakić, S. Nikolovski, and T. Dragičević, "Anti-islanding protection of PV-based micro-grids consisting of PHEVs using SVMs," *IEEE Trans. Smart Grid*, vol. 11, no. 1, pp. 483–500, Jan. 2020.

[20] H. Samet, F. Hashemi, and T. Ghanbari, "Minimum non detection zone for islanding detection using an optimal artificial neural network algorithm based on PSO," *Renew. Sustain. Energy Rev.*, vol. 59, pp. 1–18, Dec. 2014.
[21] X. R. Kong, X. Y. Xu, Z. Yan, S. J. Chen, H. M. Yang, and D. Han, "Deep learning hybrid method for islanding detection in distributed generation," *Appl. Energy*, vol. 210, pp. 776–785, Jan. 2018.
[22] S. Admasie, S. B. A. Bukhari, R. Haider, T. Gush, and C. H. Kim, "A passive islanding detection scheme using variational mode decomposition-based mode singular entropy for integrated microgrids," *Elect. Power Syst. Res.*, vol. 177, Dec. 2019, Art. no. 105983.
[23] R. Dubey, M. Popov, and S. R. Samantaray, "Transient monitoring function-based islanding detection in power distribution network," *IET Gener. Transm. Distrib.*, vol. 13, no. 6, pp. 805–813, May 2018.
[24] S. Agrawal, S. Patra, S. R. Mohanty, V. Agarwal, and M. Basu, "Use of matrix-pencil method for efficient islanding detection in static DG and a parallel comparison with DWT method," *IEEE Trans. Ind. Electron*, vol. 66, no. 11, pp. 8937–8946, Nov. 2019.
[25] R. Nale, K. Venkatanagaraju, S. Biswal, M. Biswal, and N. Kishor, "Islanding detection in distributed generation system using intrinsic time decomposition," *IET Gener. Transm. Distrib.*, vol. 13, no. 5, pp. 626–633, Dec. 2018.
[26] P. Kundur, N. J. Balu, and M. G. Lauby, *Power System Stability and Control*, vol. 7. New York, NY, USA: McGraw-Hill, 1994.
[27] H. Samet, F. Hashemi, and T. Ghanbari, "Islanding detection method for inverter-based distributed generation with negligible non-detection zone using energy of rate of change of voltage phase angle," *IET Gener. Transm. Distrib.*, vol. 9, no. 15, pp. 2337–2350, Nov. 2015.
[28] H. Samet, "Evaluation of digital metering methods used in protection and reactive power compensation of micro-grids," *Renew. Sustain. Energy Rev.*, vol. 62, pp. 260–279, Sep. 2016.
[29] N. Otsu, "A threshold selection method from gray-level histograms," *IEEE Trans. Syst., Man, Cybern., Syst.*, vol. SMC-9, no. 1, pp. 62–66, Jan. 1979.
[30] Z. Ye, A. Kolwalkar, Y. Zhang, P. Duand, and R. Walling, "Evaluation of anti-islanding schemes based on nondetection zone concept," *IEEE Trans. Power Electron.*, vol. 19, no. 5, pp. 1171–1176, Sep. 2004.
[31] J. Z. Zhu, "Optimal reconfiguration of electrical distribution network using the refined genetic algorithm," *Elect. Power Syst. Res.*, vol. 62, no. 1, pp. 37–41, 2002.
[32] A. Mohr, *Quantum Computing in Complexity Theory and Theory of Computation*, Southern Illinois Univ. Carbondale, Carbondale, IL, USA, Feb. 2014.

Hasan Khosravi received the M.Sc. degree in electrical engineering from Shiraz University. His main research interests are power quality, distributed generation, and power system protection.

Haidar Samet (Member, IEEE) received the Ph.D. degree in electrical engineering from the Isfahan University of Technology. He is currently a Professor with Shiraz University and a Postdoctoral Researcher with the Eindhoven University of Technology. His main research interest is application of DSP techniques in power systems, such as protection and power quality.

Mohsen Tajdinian received the Ph.D. degree in electrical engineering from Shiraz University. His main research interests are power system protection, power quality, and power system stability.